Essay on Magnetic-Wind Mills
Part III : Pathway for energy transfer

J.L. Duarte
Dept. Electrical Engineering (Ret.)
Eindhoven University of Technology
The Netherlands

***Abstract*—An attempt is made to describe that mechanical vibrations are not only responsible for inducing resonances in spacetime, as Einstein-Cartan-Evans theory predicts, but could also provide an interface for the transfer of energy from the quantum vacuum to a rotating shaft.**

I. Introduction

The assemblage around a magnetic-wind mill, presented in [1], seems quite unusual. Yet, it is essentially a convenient experimental setup for studying the process of scavenging energy from the quantum vacuum, as predicted by the ECE theory [2].

In this paper, based on the developments in [3], analysis is advanced through simple assumptions and straightforward equations, with the aim of showing that the mechanical vibrations observed in the setup could provide a means of transferring energy to the mill shaft.

The inventor in [1] claims a useful output power around 4kW for the magnetic flux mill. However, this power level has not been strictly measured by instruments during the demonstration, only stable operation with different load gadgets is shown. Still, taking into account other previously registered video's from the same inventor, we have no reason to doubt he is acting in good faith.

An appealing aspect of the setup is that it allows research and improvements without a completely developed design model for the flux mill. The exact power level is not essential for the developments in the next sections, the same order of magnitude is sufficient.

II. A peculiar experimental setup

The flux mill in [1] has cylindrical rotor and a hinge-like split stator around it. On the rotor's surface, which is assembled from a thin-metal can, 64 PM disks (short cylindrical-shaped permanent magnets) are fixed in helix staggering (4 rings with 16 PM disks per ring). The 2-part stator has also in total 64 PM disks (4 rings per part, 8 PM disks per split ring), facing the rotor PM's with the same magnetic polarity.

The two parts of the stator are connected by a non-rigid clip, which produces small mechanical vibrations during operation. All PM disks have the same dimensions (5mm/2mm), with a little iron filings around them to facilitate crossing when PM's meet during rotation. In addition, a flywheel is added to the rotor to increase inertia and smooth rotation.

The flux mill shaft is mechanically driven by a belt that is coupled to the shaft of a single-phase 127VAC motor (a washing-machine motor type). This AC motor is electrically fed by one of the two AC outlets of a DC/AC electronic inverter (from 12VDC to square-wave 110VAC/60Hz).

The 12VDC inlet of the electronic inverter is, in turn, powered by the DC voltage side from an alternator (a automobile starter motor/generator), while a 12VDC battery is also connected in parallel to this same DC inlet.

Finally, the alternator shaft is also coupled by a belt to the rotating shaft of the flux mill. Altogether, when excluding the 12VDC battery, we have a closed loop concerning energy circulation, where the expected prime-mover is the magnetic flux mill.

Initially, the alternator is fed by the 12VDC battery to bring all the shafts up to nominal speed (as in an automobile), and the battery is subsequently disconnected. From this moment on, there are no sustainable power sources in the setup other than the *energy available from the quantum vacuum* [2].

When the system enters stable operation, different loads are be connected to the second 110VAC electronic inverter outlet (like light bulbs, drills, electric saw, etc.), and enough energy is unfolded, as demonstrated in the video.

What concerns the external magnetic field generated in the setup from spacetime, a circularly polarized flux density is assumed [3], with general expression (in ccw convention)

$$\vec{B}_{ext} = B_S \left[\cos(\kappa z - \omega t)\vec{a}_x - \sin(\kappa z - \omega t)\vec{a}_y\right], \qquad (1)$$

where $\vec{a}_x, \vec{a}_y$ are orthonormal vectors referenced to a stationary frame, and ω the rotor shaft angular velocity. In the case of a rotor with radius r_C and height h_C, wherein n equally separated rings with η PM disks per ring are inlaid, the wavenumber κ in (1) is found to become

$$\kappa = \frac{n-1}{\eta}\,\frac{\pi}{h_C}. \qquad (2)$$

III. (Non)conservative magnetic forces

Fig. 1 shows a situation in which a PM disk is attracted/repelled by an external magnetic field, $\vec{B}_{\rm ext}\,[T]$, where the disk will be moved. As a result, work will be done in the process.

The center coordinates of the PM disk are referenced to orthonormal vectors $(\vec{a}_x, \vec{a}_y, \vec{a}_z)$, together with

$$\begin{aligned} \vec{a}_r &= \cos\phi\,\vec{a}_x + \sin\phi\,\vec{a}_y, \qquad (3)\\ \vec{a}_\phi &= -\sin\phi\,\vec{a}_x + \cos\phi\,\vec{a}_y, \end{aligned}$$

according to the convention for angle ϕ in Fig. 1.

In permanent magnets, the magnetic field arises from elementary spin dipole moments in the material [4]. As such, the PM disk is assumed to have homogeneous volumetric density of magnetic dipole moments, $M\,[Am^2/m^3]$, with $M = B_r/\mu_0$, where $B_r\,[T]$ is the remanent magnetization of the material, and $\mu_0 = 4\pi 10^{-}7\,[H/m]$ the permeability of free space.

Further, as a first-order approximation, we also consider that the external field $\vec{B}_{\text{ext}}$ in a disk volume has approximately the same value as at its center. Consequently, a PM disk, with radius R_D and height h_D, is modeled as single magnetic dipole moment, $\vec{\mu}_C$, which represents the superposition of all elementary spin dipole moments in the disk volume pointing out in the same direction, where

$$\| \vec{\mu}_C \| = \mu_C = \pi R_D^2 h_D M. \tag{4}$$

In Fig. 1, the magnetic dipole moment $\vec{\mu}_C$ with coordinates (x_C, y_C, z_C) is free to rotate with constant radius r_C and angular displacement ϕ around the axis $\vec{a}_z$. That is to say,

$$x_C = r_C \cos\phi\,,\; y_C = r_C \sin\phi \tag{5}$$

and

$$\vec{\mu}_C = \mu_C\,\vec{a}_r\,. \tag{6}$$

Superposed to ϕ, small angular disturbances, ϕ'_S, take place, being synchronized with the rotation of $\vec{\mu}_C$. These disturbances represent shaft angular vibrations, which are induced in the mechanical assembly by dynamic forces when a rotor PM disk crosses other magnets in proximity, as considered later.

In order to analyze the interaction between the magnetic moment $\vec{\mu}_S$ and the field $\vec{B}_{\text{ext}}$, the classical Lorentz force formula has to be extended with one more component as

$$\vec{F} = q\vec{E}_{\text{ext}} + q\vec{v} \times \vec{B}_{\text{ext}} + \vec{\nabla}(\vec{\mu}_C \cdot \vec{B}_{\text{ext}}). \tag{7}$$

The term $\vec{\nabla}(\vec{\mu}_C \cdot \vec{B}_{\text{ext}})$ is capable of performing work, what is not the case for $q\vec{v} \times \vec{B}_{\text{ext}}$ [4].

A research question in this discussion paper is, if the magnetic force introduced by the $\vec{\nabla}(\vec{\mu}_S \cdot \vec{B}_{\text{ext}})$ term is *conservative*. It will be the case if there is zero net work done when moving the magnetic dipole $\vec{\mu}_C$ through the field $\vec{B}_{\text{ext}}$, following the closed cyclic path $0 \le \phi \le 2\pi$. If *not*, then net energy will be taken from the external magnetic field.

IV. Mechanical vibrations meet magnetic trill

As previously mentioned, a circularly polarized magnetic flux density waveform is assumed for the external magnetic field, which is generated by resonances in spacetime. However, due to the low construction stiffness of the mill assemblage, unavoidably all kind of mechanical vibrations are induced by magnetic force perturbations. Consequently, it is to be expect that the generated external magnetic field will also present small magnitude variations, in synchronicity with the setup mechanical disturbances.

It is a basic assumption in this paper that the trilling magnetic field component in the *radial direction* is significant

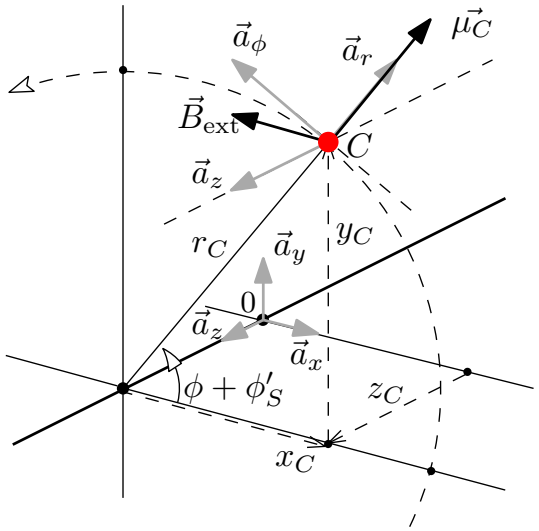

Fig. 1: Magnetic dipole moment, $\vec{\mu}_C$, representing a PM disk, free to rotate with constant radius, r_C, and small angular disturbances, ϕ'_S, in a external magnetic field $\vec{B}_{\text{ext}}$.

for energy transfer. Therefore, as an extension of (1), the external field at (x_C, y_C, z_C) is described by

$$\vec{B}_{\text{ext}} = B_{\text{ext}}\,[\cos\phi\,\vec{a}_x + \sin\phi\,\vec{a}_y]\,, \tag{8}$$

with $\phi = \omega t - \kappa z_C$, while

$$B_{\text{ext}} = B_S + B'_S \cos(\eta\phi), \tag{9}$$

where B_S and B'_S are constant, and $B'_S \ll B_S$. The term $B'_S \cos(\eta\phi)$ in (9) is a first approximation for the field magnitude vibrations, being synchronized with the changing forces when $\vec{\mu_C}$ (that models one rotor PM disk) crosses over η PM disks in a stator ring, for $0 \le \phi \le 2\pi$.

Without lost of generality, in the following $z_C \equiv 0$ is chosen for (8), meaning that the focus is just at one of the stator rings with PM's (in case, the lowest one).

A. Magnetic force components

As to (3) and (6),

$$\vec{\mu}_C = \mu_C\,[\cos\phi\,\vec{a}_x + \sin\phi\,\vec{a}_y]\,. \tag{10}$$

Defining

$$\mathcal{F} = \vec{\mu}_C \cdot \vec{B}_{\text{ext}}, \tag{11}$$

it results from (8) and (10) that

$$\mathcal{F} = \mu_C\,(B_S + B'_S \cos(\eta\phi))\,. \tag{12}$$

Correspondingly, the resulting force on the magnetic dipole moment $\vec{\mu}_C$ is obtained with reference to (7) :

$$\vec{F}_C = \vec{\nabla}\mathcal{F}. \tag{13}$$

The required gradients in (13) can be calculated as function of the angular inclination ϕ with

$$\vec{F}_C = \frac{\partial\mathcal{F}/\partial\phi}{\partial x_S/\partial\phi}\vec{a}_x + \frac{\partial\mathcal{F}/\partial\phi}{\partial y_S/\partial\phi}\vec{a}_y, \tag{14}$$

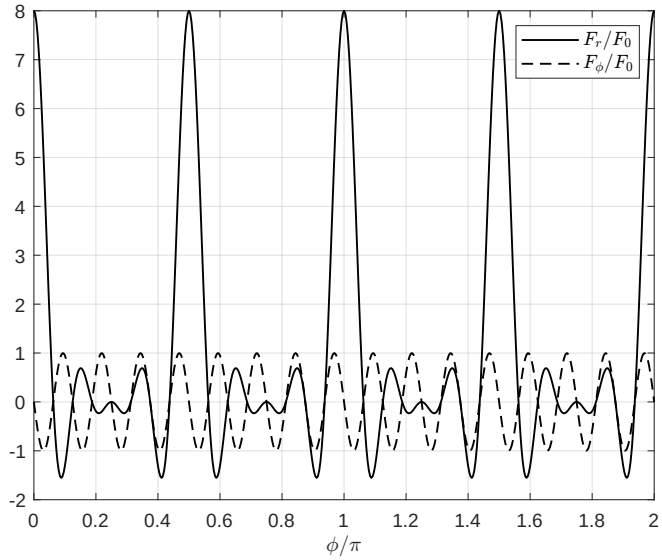

Fig. 2: Radial (F_r) and tangential (F_ϕ) forces. Normalized Eqs.(20)-(21) with $\eta = 16$.

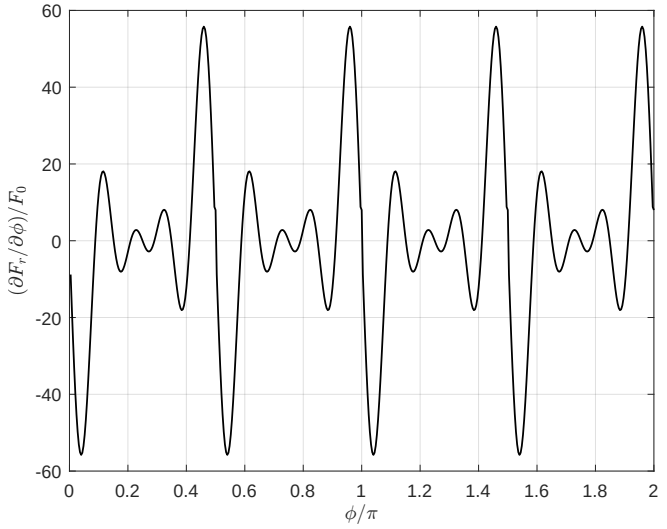

Fig. 3: Rate-of-change of the radial force in Fig.(3). Normalized Eq.(24) with $\eta = 16$.

where, from (12),

$$\frac{\partial \mathcal{F}}{\partial \phi} = -\eta \mu_C B'_S \sin(\eta\phi), \tag{15}$$

and, in regard to (5),

$$\begin{aligned} \partial x_S/\partial\phi &= -r_C \sin\phi, \\ \partial y_S/\partial\phi &= r_C \cos\phi. \end{aligned} \tag{16}$$

Respecting cylindrical coordinates, $\vec{F}_C$ is given by

$$\begin{aligned} \vec{F}_C &= F_r\,\vec{a}_r + F_\phi\,\vec{a}_\phi, \\ F_r &= F_x\cos\phi + F_y\sin\phi, \\ F_\phi &= -F_x\sin\phi + F_y\cos\phi. \end{aligned} \tag{17}$$

After substitution of (16) into (14), it follows from (17) that

$$\begin{aligned} F_r &= \frac{\partial \mathcal{F}}{\partial\phi}\frac{\cos\phi}{-r_C\sin\phi} + \frac{\partial \mathcal{F}}{\partial\phi}\frac{\sin\phi}{r_C\cos\phi} \\ &= -\frac{2}{r_C}\frac{\partial \mathcal{F}}{\partial\phi}\frac{\cos(2\phi)}{\sin(2\phi)}, \end{aligned} \tag{18}$$

$$\begin{aligned} F_\phi &= -\frac{\partial \mathcal{F}}{\partial\phi}\frac{\sin\phi}{-r_C\sin\phi} + \frac{\partial \mathcal{F}}{\partial\phi}\frac{\cos\phi}{r_C\cos\phi} \\ &= \frac{2}{r_C}\frac{\partial \mathcal{F}}{\partial\phi}, \end{aligned} \tag{19}$$

which leads to, in view of (15),

$$F_r = F_0\frac{\sin(\eta\phi)\cos(2\phi)}{\sin(2\phi)}, \tag{20}$$

$$F_\phi = -F_0\sin(\eta\phi), \tag{21}$$

with

$$F_0 = 2\frac{\eta\mu_C B'_S}{r_C}. \tag{22}$$

A plot of (20)-(21) for $\eta = 16$ is shown in Fig. 2.

B. Rotor angular vibration

The trilling angle, ϕ'_S in Fig. 1, is due to the superposition of a variety of mechanical perturbations with multiple causes. Be that as it may, another primary assumption is to consider that the angular trill component in the rotor *tangential* direction, which is *dynamically* induced by the rate-of-change of *radial forces* in the assemblage, is significant for energy transfer.

Since stator and rotor radial forces are similar, an expression for infinitesimal increments of ϕ'_S is written as

$$d\phi'_S = \lambda\frac{\partial F_r}{\partial\phi}d\phi, \tag{23}$$

where λ is a constant of proportionality, intrinsic to the assemblage mechanical rigidity, and, with reference to (20),

$$\frac{\partial F_r}{\partial\phi} = -F_0\left[2\frac{\sin(\eta\phi)}{\sin^2(2\phi)} - \eta\frac{\cos(\eta\phi)\cos(2\phi)}{\sin(2\phi)}\right]. \tag{24}$$

A plot of (24) for $\eta = 16$ is shown in Fig. 3.

Due to (23), the rotor trilling angle is determined with

$$\phi'_S = \lambda\int_0^\phi \frac{\partial F_r}{\partial\phi}d\phi\,, \tag{25}$$

and its peak-to-peak magnitude, $\Delta\phi'_S$, ascertained from

$$\Delta\phi'_S = \max(\phi'_S) - \min(\phi'_S)\,,\ 0 \le \phi \le 2\pi. \tag{26}$$

C. Energy increments

Work is done by the rotor tangential force F_ϕ upon the magnetic dipole $\vec{\mu_C}$ at each linear increment $d\phi'_S$. Since $\vec{\mu_C}$ is located with radius r_C around a pivot axis, a infinitesimal energy increment equal to

$$dQ'_S = F_\phi\, r_C\, d\phi'_S \tag{27}$$

is, therefore, added to the rotating system parts.

In relation to (19) and (23), (27) is found to become

$$dQ'_S = 2\lambda\left(\frac{\partial \mathcal{F}}{\partial\phi}\right)\left(\frac{\partial F_r}{\partial\phi}\right)d\phi. \tag{28}$$

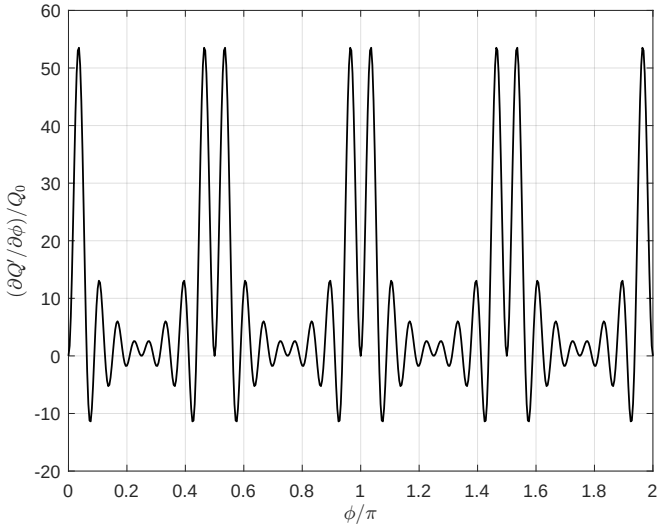

Fig. 4: Energy transfer trill as function of the shaft angular position. Normalized Eq.(29) with $\eta = 16$.

Taking (15) and (24) into account, after some manipulations it results from (28) that

$$\frac{\partial Q'_S}{\partial\phi} = Q_0 \frac{\sin(\eta\phi)}{\sin(2\phi)} \left[2\frac{\sin(\eta\phi)}{\sin(2\phi)} - \eta\cos(\eta\phi)\cos(2\phi) \right] \quad (29)$$

with

$$Q_0 = 8\frac{\lambda(\eta\mu_C B'_S)^2}{r_C}\,. \quad (30)$$

A plot of (29) for $\eta = 16$ is shown in Fig. 4. It can be seen that the average of $\partial Q'_S/\partial\phi$ is not zero. As a consequence,

$$Q'_S = \int_0^{2\pi} \frac{\partial Q'_S}{\partial\phi} d\phi \; > \; 0\,, \quad (31)$$

meaning that after each complete turn, a net mechanical energy increase equal to Q'_S is brought into the rotor shaft.

V. Numerical example

The primary parameter for quantification of the analysis in the previous sections is B'_S, the trilling magnitude of the magnetic flux generated from spacetime.

If a working setup is available for open research, it should be possible to measure the value of B'_S. Alternatively, if $\Delta\phi'_S$ is measured (the peak-to-peak magnitude of the rotor angular trill), the value of B'_S can be fetched by try-and-error iterations, following the procedure below. Based on the value of B'_S, all the other coefficients for the previous equations can be obtained.

The geometrical dimensions from Table 1 are applied in the sequence, being similar to the ones in the setup of [1].

For instance, if it is desired to have a flux mill that delivers P =500W mechanical power out of the rotor shaft at 1000rpm, the necessary total mechanical energy per turn, say Q_Σ, at $\omega = \frac{2\pi}{60}1000$ [rad/s], should be

$$Q_\Sigma = P/\omega = 4.77\,[J]. \quad (32)$$

TABLE I: Parameters and geometrical dimensions

Parameter		Value	Description
B_r	[T]	1.42	remanent magnetization NFeB 52
R_D	[mm]	2.5	PM disk radius
h_D	[mm]	2.0	PM disk height
r_C	[mm]	40	rotor radius
h_C	[mm]	45	rotor height
n	[-]	4	number of rotor rings with PM's
η	[-]	16	number of PM's per ring
P	[W]	500	rotor mechanical output power
rpm	[turns/min]	1000	shaft rotation speed

Since there are 64 (= $n\,\eta$) PM disks inlaid on the rotor, the required energy increment per turn per each PM disk will be

$$Q'_S = \frac{Q_\Sigma}{64} = 74.6\,[mJ]. \quad (33)$$

Regarding (29), it results for $\eta = 16$ that

$$\frac{Q'_S}{Q_0} = \frac{1}{Q_0}\int_0^{2\pi} \frac{\partial Q'_S}{\partial\phi} d\phi = 50.27\,, \quad (34)$$

$$\Rightarrow Q_0 = \frac{1}{50.27} Q'_S = 0.0015. \quad (35)$$

To proceed, an attempt value for B'_S is needed. Let's try B'_S = 80mT, which is a small quantity if, for instance, the remanent flux density of the magnet type in Table 1 (B_r = 1.42T) is taken as reference.

Continuing,

$$F_0 = 2\frac{\eta\mu_C B'_S}{r_C} = 2.90\,, \quad (36)$$

$$\lambda = \frac{1}{8}\frac{r_C}{(\eta\mu_C B'_S)^2} Q_0 = 0.0022\,, \quad (37)$$

and the trilling angle ϕ'_S can be calculated from (25):

$$\phi'_S = \lambda \int_0^{\phi} \frac{\partial F_r}{\partial\phi} d\phi\,,\; 0 \le \phi \le 2\pi\,, \quad (38)$$

as shown in Fig. 5.

At last, inspecting Fig. 5, we get with (26) that

$$\Delta\phi'_S = 0.0067\pi = 1.20^o\,, \quad (39)$$

confirming that transfer of energy from the quantum vacuum could be realized based on small mechanical vibrations in the structure of the flux mill.

Fig. 6 shows the sensitivity of $\Delta\phi'_S$ with respect of B'_S. The higher B'_S, the smaller the mechanical vibrations needed for generating the same power of 500W at 1000rpm.

VI. Conclusion

Applying the concepts of [3] to the situation of [1], it is hypothesized that mechanical vibrations and trilling magnetic flux are matched in a magnetic-wind mill. The underlying premises are: (a) the magnitude of the external magnetic flux, created from resonance in spacetime, bears a *radial* trilling component due to the low rigidity of the mechanical assembly, and (b) the *tangential* rotor angular vibration has a component proportional to the rate-of-chance of dynamic *radial* forces. In this way, a path is given for describing the transfer of energy from the quantum vacuum to the mill shaft.

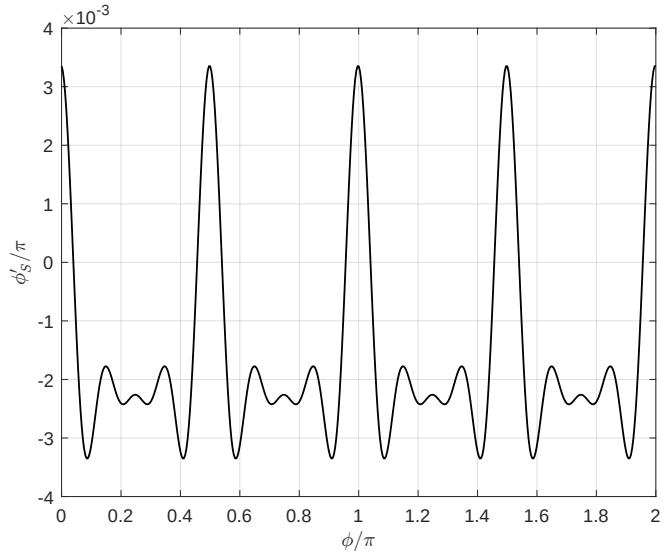

Fig. 5: Angular rotor disturbances. Eq.(25) with $\eta = 16$ and B'_S = 80mT.

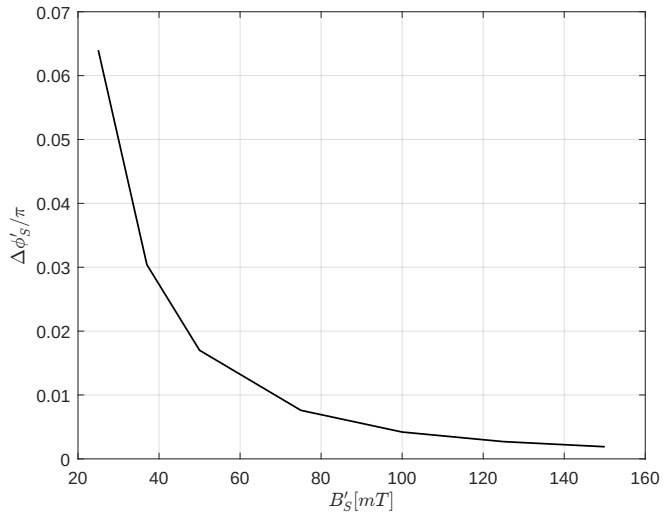

Fig. 6: Peak-to-peak angular vibration magnitude superposed on the rotor shaft , as function of trill in the magnetic flux magnitude. Eq.(26) with η =16 and P =500W at 1000rpm.

A numerical example is provided to check whether the calculated peak-to-peak magnitude of the rotor's angular vibration has a small realistic value. And it is the case.

REFERENCES

[1] *Dicas do Leao, Self-sustained energy generator 4000W*, video posted on July 24th, 2023, https://www.youtube.com/watch?v=IBV8Pg0RcII

[2] H. Eckardt, *Einstein-Cartan-Evans Unified Field Theory*, Feb. 2022, ISBN-13: 978-3754949474

[3] J.L. Duarte, *Essay on magnetic-wind mills, Part II : Staying power from spacetime*, Feb 2023, https://aias.us/documents/otherPapers/|

[4] J.A. Barandes, *Can magnetic forces do work?*, July 2023, https://arxiv.org/abs/1911.08890

First appeared: November 9th, 2024

J.L. Duarte
magnetogenesis@proton.me
https://github.com/JLDuarte55/magnetogenesis